Journal of Applied Polymer Science

Preparation of Vinyl Amine-*co*-Vinyl Alcohol/Polysulfone Composite Membranes and Their Carbon Dioxide Facilitated Transport Properties

Alsamani A. M. Salih, Chunhai Yi, Jiayang Hu, Lijuan Yin, Bolun Yang
School of Chemical Engineering and Technology, Xi'an Jiaotong University, Xi'an Shaanxi 710049, China
Correspondence to: C. Yi (E-mail: chyi@mail.xjtu.edu.cn)

ABSTRACT: A vinyl amine–vinyl alcohol copolymer (VAm–VOH) was synthesized through free-radical polymerization, basic hydrolysis in methanol, acidic hydrolysis in water, and an anion-exchange process. In the copolymer, the primary amino groups on the VAm segment acted as the carrier for CO_2-facilitated transport, and the vinyl alcohol segment was used to reduce the crystallinity and increase the gas permeance. VAm–VOH/polysulfone (PS) composite membranes for CO_2 separation were prepared with the VAm–VOH copolymer as a selective layer and PS ultrafiltration membrane as a support. The membrane gas permselectivity was investigated with CO_2, N_2, and CH_4 pure gases and their binary mixtures. The results show that the CO_2 transport obeyed the facilitated transport mechanism, whereas N_2 and CH_4 followed the solution–diffusion mechanism. The increase in the VAm fraction in the copolymer resulted in a carrier content increase, a crystallinity increase, and intermolecular hydrogen-bond formation. Because of these factors, the CO_2 permeance and CO_2/N_2 selectivity had maxima with the VAm fraction. At an optimum applied pressure of 0.14 MPa and at an optimum VAm fraction of 54.8%, the highest CO_2 permeance of 189.4 GPU [1 GPU = 1×10^{-6} cm^3(STP) cm^{-2} s^{-1} $cmHg^{-1}$] and a CO_2/N_2 selectivity of 58.9 were obtained for the CO_2/N_2 mixture. The heat treatment was used to improve the CO_2/N_2 selectivity. At an applied pressure of 0.8–0.92 MPa, the membrane heat-treated under 100°C possessed a CO_2 permeance of 82 GPU and a CO_2/N_2 selectivity of 60.4, whereas the non-heat-treated membrane exhibited a CO_2 permeance of 111 GPU and a CO_2/N_2 selectivity of 45. After heat treatment, the CO_2/N_2 selectivity increased obviously, whereas the CO_2 permeance decreased.
 J. Appl. Polym. Sci. **2014**, *131*, 40043.

KEYWORDS: copolymers; crystallization; membranes

Received 28 April 2013; accepted 7 October 2013
DOI: 10.1002/app.40043

INTRODUCTION

Carbon dioxide is an impurity that must be removed from mixtures with light gases, such as CH_4, N_2, and H_2, and the scale of these separation is enormous.[1–4] Currently, CO_2 is removed from gas mixtures mainly by absorption, adsorption, and membrane technology. Compared with adsorption and absorption, membrane technology has the advantages of low capital cost, simplicity, low energy consumption, and compact structure.[5] However, for membrane separation, the preparation of membranes with both a high CO_2 permeance and a high selectivity is always the most important challenge, and this limits its industrial application.

Among the membranes for CO_2 separation, fixed site carrier (FSC) membranes have been regarded as the most promising membranes for CO_2 separation.[3,6–9] In FSC membranes, carriers such as amino groups and pyridine groups reacted reversibly with CO_2. Because of the reversible complex reaction between CO_2 and the carrier, FSC membranes showed both a high CO_2 permeance and a high selectivity. In the meantime, the carrier was fixed to the polymeric substrate by chemical bonds, and this leads to a very good stability.

FSCs membrane were first reported by Yoshikawa et al.[10,11] They synthesized a polymeric membrane having pyridine groups or amino groups and confirmed the acid–base reversible reaction between CO_2 and fixed carriers. The high permselectivity and good stability of FSC membranes has aroused a lot of interest. Among these studies, amino-group-containing FSC membranes have been investigated extensively. Hägg and coworkers[8,12–14]and Wang and coworkers[6,15–17] reported several kinds of poly(vinyl amine) (PVAm) membranes with primary amino groups for CO_2-facilitated transport. Feng et al.[18] reported poly(2-dimethylamino ethyl methacrylate) membranes containing tertiary amine as a carrier. In addition the amino and pyridine groups, Wang and coworkers[19–22] found that the carboxyl acid ion could also be used as a carrier for CO_2 permeation. They prepared a poly(*N*-vinyl-γ-sodium aminobutyrate) membrane and a poly(*N*-vinyl-γ-sodium aminobutyrate-*co*-sodium acrylate) membrane through the hydrolysis of poly(vinyl pyrrolidone) (PVP) and a *N*-vinyl pyrrolidone–

acrylamide copolymer. In these research, Wang et al.[22] discovered that H_2O played a very important role in CO_2 permeation through FSC membranes. In the existence of a weak base group, CO_2 could react with H_2O and form an HCO_3^- ion.

An approach of FSC membranes is the preparation of a polymeric blend membrane. Matsuyama et al.[7] prepared a homogeneous poly(ethylene imine) (PEI)–poly(vinyl alcohol) (PVA) blend membrane with a CO_2/N_2 selectivity as high as 230. Hägg et al.[13] reported a PEI–PVA blend membrane with a CO_2 permeance of 200–300 GPU [1 GPU = 1×10^{-6} cm^3(STP) cm^{-2} s^{-1} $cmHg^{-1}$] and CO_2/N_2 and CO_2/CH_4 selectivities of 45 and 160, respectively. Cai et al.[16] also prepared polyallylamine–PVA blend membranes with a CO_2 permeance of 24.6 GPU and a CO_2/N_2 selectivity of 80. From the studies mentioned previously, we concluded that good stability and mechanical properties were obtained by the entanglement of an FSC membrane material chain with PVA chains.[7]

In our previous research,[15] we prepared a PVAm–PEG blend membrane. We found that the blend membrane had a better permselectivity than a pure PVAm membrane, although the carrier content of the blend membrane was much lower. This was attributed to a drop in the polymer crystallinity. As revealed in other polymeric gas-separation membranes, the formation of crystals is deleterious to gas permeation. The formation of crystals in polymer membrane is deleterious because they act as impermeable obstacles.[23] FSC membrane materials often have a high concentration of polar groups, including amino groups and pyridine groups. Generally, polar groups in a polymer improve the polymer chain-packing efficiency and promote chain crystallization.[24] The blending of FSC membrane materials with other polymers is an effective method for reducing the crystallinity, and it leads to an improvement in the membrane permselectivity.[16]

Synthesizing copolymers is another way to improve the membrane permselecitvity and its mechanical properties. Feng et al.[25,26] prepared different kinds of poly(amide-*block*-ether oxide) copolymer membranes. Okamoto et al.[27] prepared poly(-ether imide) segmented copolymer membranes. Because of the good affinity of CO_2 to PEO segments, these copolymers exhibited a higher CO_2 permeability. However, there have been few reports on copolymers for CO_2-facilitated transport. Wang et al.[20] prepared a poly(*N*-vinyl-γ-sodium aminobutyrate-*co*-sodium acrylate) membrane by the hydrolysis of an *N*-vinyl pyrrolidone–acrylamide copolymer. The results show that the copolymer had better performance than the poly(*N*-vinyl-γ-sodium aminobutyrate) membrane.

In this study, to improve the FSC membrane permselectivity, a vinyl amine–vinyl alcohol copolymer (VAm–VOH) was developed. In this copolymer, the primary amino groups on the vinyl amine (VAm) segment reacted with CO_2 and facilitated the transport of CO_2. The introduction of vinyl alcohol (VOH) segments into the polymer decreased the regularity of the polymer chain, and this reduced the crystallinity. Hydroxyl groups cannot react with CO_2. Therefore, hydroxyl groups could not act as carriers for CO_2 and did not contribute to the facilitated transportation of CO_2. However, hydroxyl groups have a good affinity with CO_2.[28] This good affinity increased the CO_2 solubility and thus improved its solution–diffusion transport. The VAm–VOH copolymer facilitated both FSC-based carrier-facilitated transport and the solution–diffusion transport of CO_2. The composite membrane was prepared with VAm–VOH as a selective layer and a polysulfone (PS) ultrafiltration membrane as a support. The effects of the copolymer composition and heat treatment on the membrane structure and gas permselectivity were investigated.

EXPERIMENTAL

Materials

N-Vinyl formamide (NVF) and vinyl acetate (VAc) were purchased from Sigma-Aldrich Corp. (China). Both monomers were distilled *in vacuo* to remove the stabilizer before use. 2,2′-Azobis(2-methylpropionamide) dihydrochloride (AAPH) was purchased from J&K Chemical, Inc. (China) and was recrystallized from ethanol. A macroporous, strong-base, anion-exchange resin was supplied by Xi'an Chemical Reagent (China). The PS ultrafiltration membrane, with an average cutoff molecular weight of 6000, was supplied by Vontron Technology Co., Ltd. (China). Methanol and KOH (analytical grade) were purchased from Aladdin Industrial, Inc. (China) and were used without further purification.

Synthesis of VAm–VOH

The synthesis of the VAm–VOH copolymer included four steps: free-radical polymerization, basic hydrolysis in methanol, acidic hydrolysis in water, and ion exchange. The synthetic procedure is shown in Figure 1 and is described in detail as follows: two monomers and a certain amount of initiator (AAPH) were dissolved in methanol. Then, the polymerization was carried out in a flask equipped with a stirrer at 60 ± 2°C for 5 h under a nitrogen atmosphere. After polymerization, the NVF—VAc copolymer solution, a colorless viscous gel-like liquid was obtained. Then, a certain amount of KOH dissolved in methanol was added to the flask. The hydrolysis was carried out at 60 ± 2°C for 10 min. During this process, NVF–VAc was hydrolyzed, and this resulted in an NVF–VOH copolymer. Thereafter, the resulting white solid (NVF–VOH copolymer) was dissolved in deionized water to make a 10 wt % solution. According to ref. 29, a certain concentration of hydrochloric acid was added to the flask, and acidic hydrolysis was carried out at 60 ± 2°C for 3.5 h. After hydrolysis, the resulting polymer chloride (VAm–VOH·HCl) was poured into a large quantity of ethanol to precipitate a white deposit. After it was dried in a vacuum oven at 60°C for 48 h, the white deposit was dissolved in a certain amount of deionized water. The polymer solution was mixed with an excess of the macroporous, strong-base, anion-exchange resin with stirring for 4 h. Finally, the VAm–VOH aqueous solution was obtained after one centrifugation.

The VAm segment fraction (x) was calculated as follows:

$$x = \frac{n_{(\text{vinyl amine})}}{\left[n_{(\text{vinyl amine})} + m_{(\text{vinyl alcohol})}\right]}$$

where $n_{(\text{vinyl amine})}$ and $m_{(\text{vinyl alcohol})}$ represent the moles of VAm segments and VOH segments, respectively, in the copolymer.

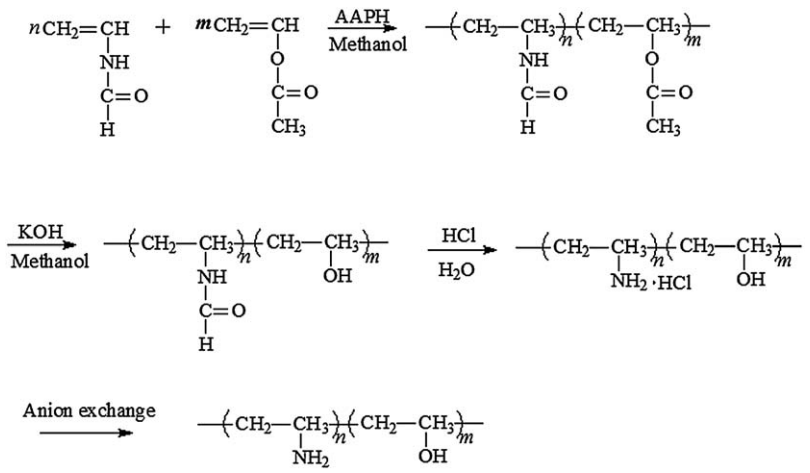

Figure 1. Syntheses of the VAm–VOH copolymer.

Composite Membrane Preparation

The VAm–VOH/PS composite membrane was prepared by knife casting technology. The PS support membrane was modified by being dipped into a sodium dodecyl sulfate aqueous solution (2 g/L) for 24 h to get rid of the dust and hydrophobic pollutant on the membrane. After it was washed with deionized water, the PS support membrane was dried at room temperature for 24 h and fixed to a glass plate. A VAm–VOH solution with a concentration of 2 wt % was cast on the PS support with a knife casting applicator; this was followed by drying at 30°C and 40% relative humidity in an climate chamber (CTHI 150B, China) for at least 24 h. The formatted membrane had a dense layer of 4.8–5 μm.

We heat-treated the dried membrane at different temperatures (from 80 to 110°C) by putting the dried composite membranes in an oven for 2 h. Then, the heat-treated membranes were cooled down to room temperature and stored in a climate chamber at 30°C and 40% relative humidity.

Characterization and Measurement

The Fourier transform infrared (FTIR) spectra of the VAm–VOH copolymer were recorded with Nicolet Avatar 360 instrument with a resolution of 4 cm^{-1}. The samples were diluted by spectral, pure-grade KBr and pressed as disks. X-ray diffraction (XRD) spectroscopy was applied to investigate the crystallinity of the VAm–VOH copolymers with a PANalytical X'PERT PRO Super XRD system with a Cu Kα radiation source ($\lambda = 1.5406$ Å) at 40 kV and 40 mA over a 2θ range of 5–80°. We prepared XRD sample films with equal thicknesses by drying the copolymer under the same temperature and humidity as used in composite membrane preparation. The crystallinity of the polymer was calculated as the ratio of peak areas assigned to the crystalline polymer to the total peak area:[30]

$$\text{Crystallinity} = \frac{A_c}{A_t}$$

where A_c is the area of the crystalline phase and A_t is the total peak area.

The gas-permeation properties of the membranes was measured by a set of test apparatus with CO_2, N_2, and CH_4 pure gases and their mixtures. The testing apparatus had the same structure as was reported in ref. 16. The feed gas flow rate was set as 400–450 mL/min, and the sweep gas flow rate was set as 90–100 mL/min. The feed gas pressures ranged from 0.1 to 1.5 MPa, whereas the downstream pressure was maintained at approximately atmospheric pressure. The effective area of the composite membranes used in the test cell was 19.26 cm^2. Before contacting the membrane, both the feed gas and the sweep gas (H_2) were humidified by passage through bottles containing water. The outlet sweep gas composition was analyzed by a gas chromatograph equipped with a thermal conductivity detector (HP4890, Porapak N). The permeation fluxes of CO_2, N_2, and CH_4 were calculated from the sweep gas flow rate and its composition. The permeation rate and selectivity are given by

$$R_i = N_i/\Delta P_i, \alpha_{A/B} = R_A/R_B \quad (1)$$

where R_i is the gas permeance of component (i), N_i is flux, ΔP_i is the pressure difference between upstream and downstream side of the membrane, $\alpha_{A/B}$ is the selectivity, R_A, R_B are the permeances of component A and B.

RESULTS AND DISCUSSION

Characterization of the VAm–VOH Copolymer

Figure 2 shows the FTIR spectra of the NVF–VAc and VAm–VOH copolymers. In the NVF–VAc spectra, the peak observed at 1245 cm^{-1} corresponded to the C—O—C stretching vibrations of ester groups.[31] The pronounced absorption band at 3278 cm^{-1} belonged to NH stretching vibrations of the amide group. The peak at 1693 cm^{-1} belonged to the C=O stretching vibrations of the amide group. As for the VAm–VOH copolymer, the characteristic absorptions of NVF–VAc, νC—O—C at 1242 cm^{-1}, and νC=O at 1693 cm^{-1} disappeared. The pronounced absorption band at 3300–3500 cm^{-1} corresponded to the NH stretching vibrations of the amino group and the OH stretching vibrations of the hydroxyl group. The absorption band at 1635 cm^{-1} belonged to the NH bending vibrations of the amino group.[32] Thus, the previous analysis confirmed the structure of the developed VAm–VOH membrane material.

The crystallinities of VAm–VOH with different VAm fractions are shown in Table I. As shown in Table I, the crystallinity increased with increasing VAm fraction. The VAm segments had

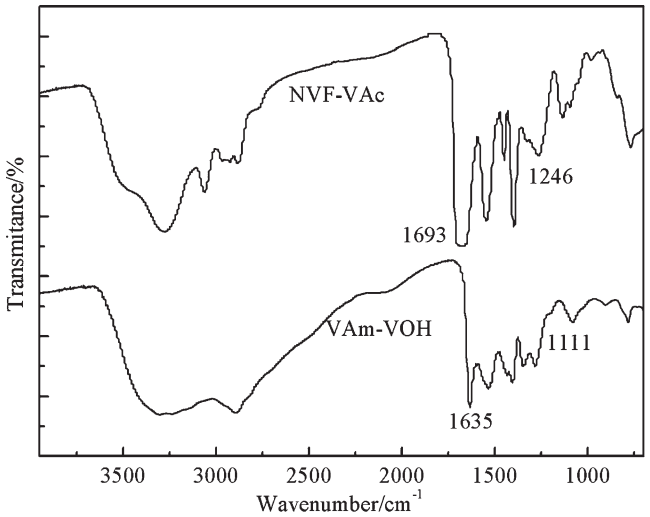

Figure 2. FTIR spectra of VAm–VOH and NVF–VAc.

Table I. The crystallinity of VAm-VOH with different VAm fraction

VAm fraction	11.8%	54.8%	64.5%	73.8%	91.6%
Crystallinity	8.4%	9.7%	9.8%	10.2%	15%

strong polar groups (primary amino groups), and this led to a strong tendency to crystallize. However, crystallization needs a regularly repeating structure of polymer chain. When the VOH segments were introduced into the polymer chain, the chain regularity decreased, and thus, the crystallization was inhibited.

Morphology of the VAm–VOH/PS Membranes

Figures 3 and 4 show the surface and cross-sectional images of the VAm–VOH/PS membrane. We observed that the separation layer of the composite membrane was dense and smooth. The thickness of the dense separation layer was about 4.8–5.0 μm.

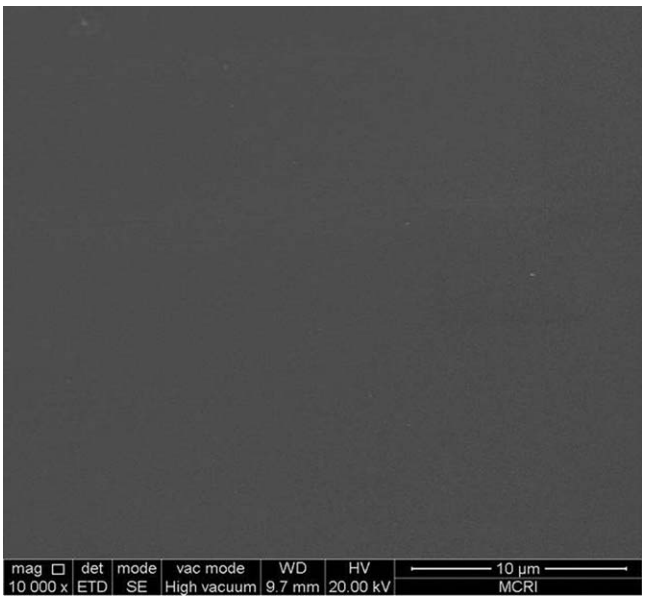

Figure 3. Surface morphology of the VAm–VOH/PS membrane.

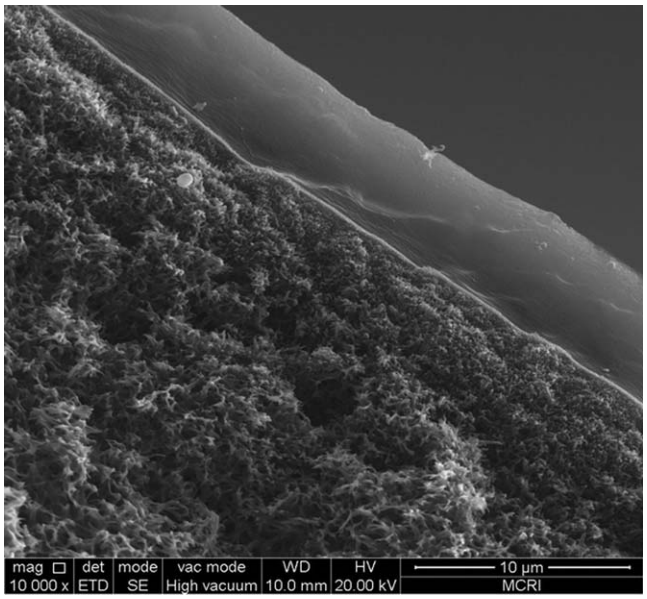

Figure 4. Cross-sectional morphology of the VAm–VOH/PS membrane.

Effects of the Membrane Composition

In this study, six kinds of VAm–VOH copolymers with different VAm fractions were prepared. As a copolymer, the composition of VAm–VOH affected not only the carrier concentration in the membranes but also the aggregation of polymer chain. As shown in Table I, the crystallinity increased with the increasing VAm fraction, so it was necessary to investigate the effects of the copolymer composition on the membrane structure and permselectivity.

Figures 5 and 6 show the CO_2/N_2 permselectivity of the VAm–VOH/PS membranes with different VAm fractions at four feed gas pressures. As shown in Figure 5, the CO_2 permeance had a maximum value against the VAm fraction in the copolymer. The membrane with a VAm fraction of 54.8% displayed the highest CO_2 permeance at pressures of 0.14–1.11 MPa.

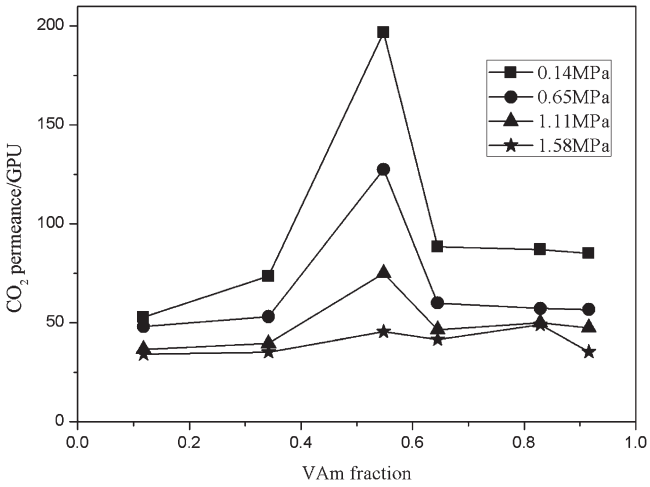

Figure 5. Effect of the copolymer composition on the CO_2 and N_2 permeances as tested with a CO_2/N_2 gas mixture (20 vol % CO_2 and 80 vol % N_2).

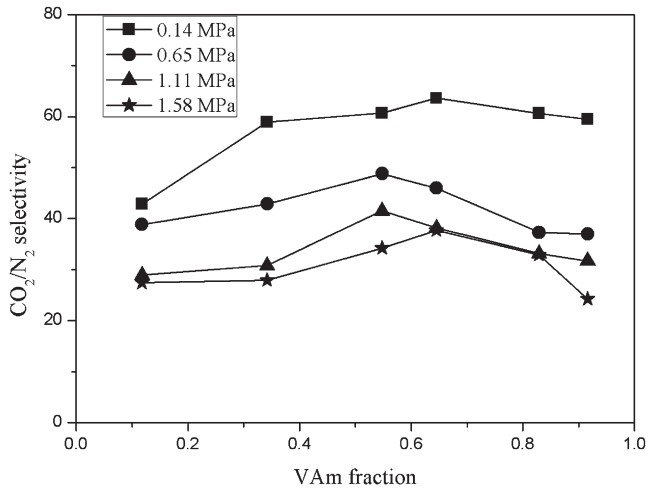

Figure 6. Effect of the copolymer composition on the CO_2/N_2 selectivity as tested with a CO_2/N_2 gas mixture (20 vol % CO_2 and 80 vol % N_2).

However, at a high pressure (1.58 MPa), the effect of the copolymer composition on the gas permselectivity could be ignored. As shown in Figure 6, the CO_2/N_2 selectivity also showed a maximum against the VAm fraction. The membrane with a VAm fraction of 54.8–64.5% exhibited the maximum CO_2/N_2 selectivity.

There were three factors that affected the significant variation of CO_2/N_2 permselectivity over the copolymer composition: carrier content, crystallization, and formation of intermolecular hydrogen bonds. Among these factors, the carrier content was a positive factor, whereas the crystallization and formation of intermolecular hydrogen bonds were negative factors.

In the VAm–VOH/PS membranes, the primary amino groups, which existed only in the VAm segments, acted as the carriers for CO_2 permeation. Numerous studies have shown that the amino group can react with CO_2 reversibly and facilitate the transport of CO_2.[3,6,16,32–34] The carrier content increased with

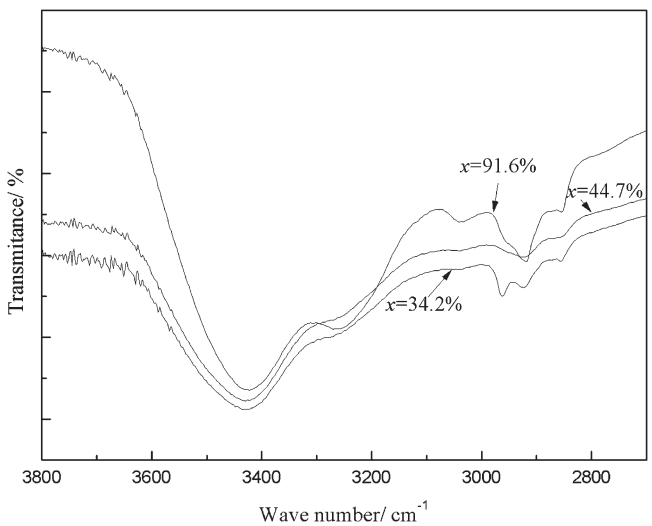

Figure 7. FTIR spectra of the VAm–VOH copolymer.

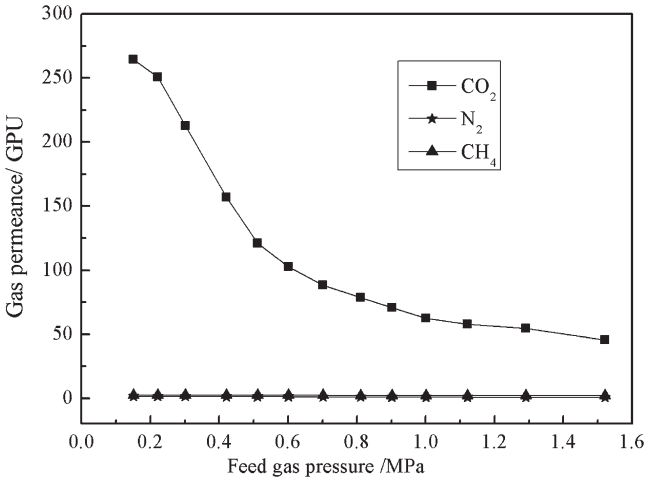

Figure 8. Effects of the feed gas pressure on the CO_2, N_2, and CH_4 permeances of the VAm–VOH/PS membrane with a 54.8% VAm fraction as tested with pure gases.

increasing VAm fraction, which was beneficial for CO_2 permeation:

$$CO_2 + R-NH_2 \rightleftharpoons R-NH_2^+ - COO^-$$

$$R-NH_2^+ - COO^- + R-NH2 \rightleftharpoons R-NH-COO^- + R-NH_3^+$$

One of the negative factors was crystallization. As shown in Table I, the crystallinity of the copolymer increased with increasing VAm fraction. The crystals that formed acted as impermeable obstacles, and this led to a low permeability. As for the fixed carrier membrane, crystallization led not only to a decrease in the effective permeation area but also to a decrease in the effective carrier content.[15] Therefore, crystallization was harmful for CO_2 permeation.

Another negative factor was the formation of hydrogen bonds between the amino groups. Yuan et al.[35] found that hydrogen bonds could be formed between primary groups in

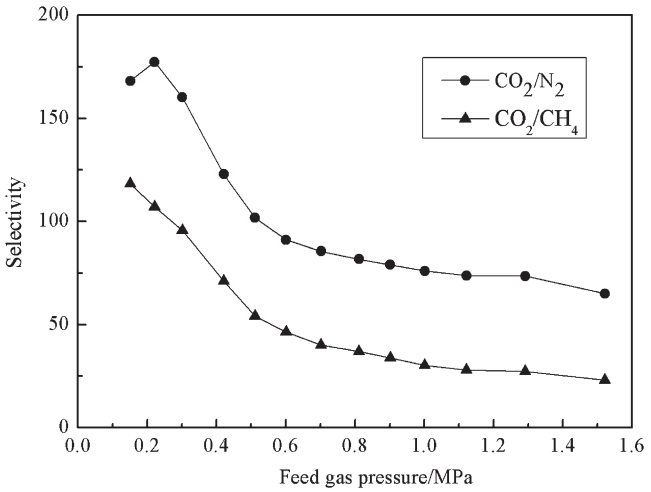

Figure 9. Effects of the feed gas pressure on the CO_2/N_2 and CO_2/CH_4 selectivity of the VAm–VOH/PS membrane with a 54.8% VAm fraction tested with pure gases.

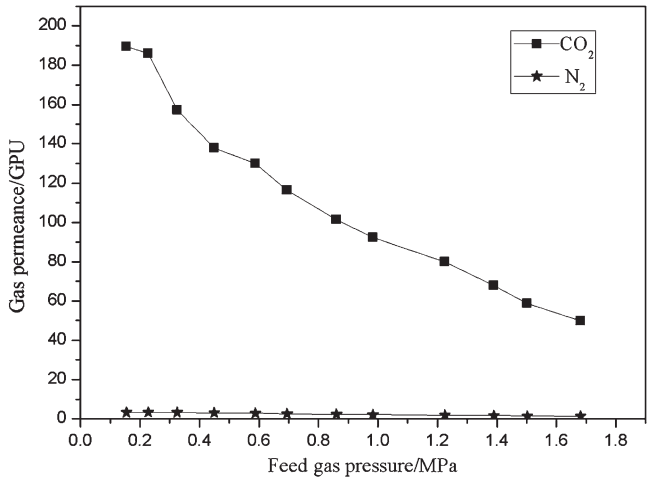

Figure 10. Effects of the feed gas pressure on the CO_2 and N_2 permeances of the VAm–VOH/PS membrane with a 54.8% VAm fraction as tested with a CO_2/N_2 mixture (20 vol % CO_2 and 80 vol % N_2).

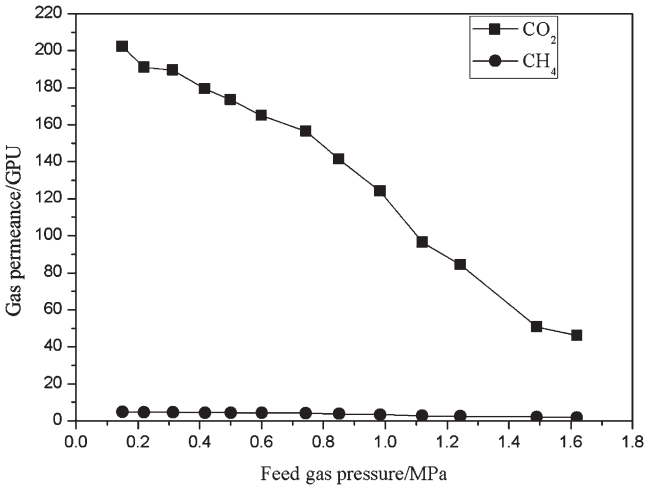

Figure 12. Effects of the feed gas pressure on the CO_2 and CH_4 permeances of the VAm–VOH/PS membrane with a 54.8% VAm fraction tested with a CO_2/CH_4 gas mixture (10 vol % CO_2 and 90 vol % CH_4).

membranes. As shown in Figure 7, the absorption bands at 3300–3500 cm^{-1} belonged to the NH stretching vibrations of amino groups. Compared with the copolymer with a low VAm fraction ($x = 0.34$ and 0.45), a small shift toward lower wave numbers was observed for the copolymer with a high VAm fraction ($x = 0.92$). This phenomenon indicated that there were hydrogen bonds formed between the amino groups.[36] The function of hydrogen bonding is similar to crosslinking and can lead to a decline in the carrier mobility. With the increase in the VAm fraction, the amino group concentration in the membrane increased. The increase in the amino group concentration resulted in the formation of more intermolecular hydrogen bonds and a drop in the CO_2 permeance.

As a net result of the three factors, both the CO_2 permeance and CO_2/N_2 selectivity had maxima against the VAm fraction. At low VAm fractions ($x = 11.8$–54.8%), the increase in the carrier content was the dominating factor. With increasing VAm fraction, the carrier content increased, and this resulted in an improvement in the CO_2/N_2 permselectivity. On the contrary, at a high VAm fraction ($x > 54.8\%$), because of the crystallization and intermolecular hydrogen bonding, the CO_2/N_2 permselectivity decreased with increasing VAm fraction. On the basis of the previous discussion, it was indicated that the VAm fraction of 54.8% was the optimal copolymer composition. Therefore, the copolymer with the VAm fraction of 54.8% was used in the following studies.

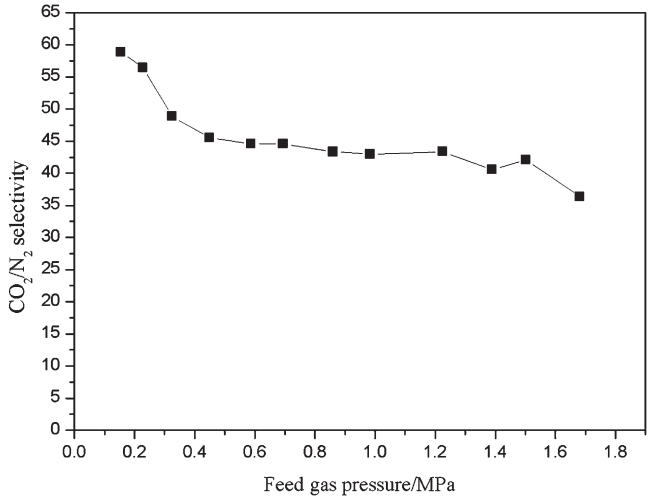

Figure 11. Effects of the feed gas pressure on the CO_2/N_2 selectivity of the VAm–VOH/PS membrane with a 54.8% VAm fraction as tested with a CO_2/N_2 mixture (20 vol % CO_2 and 80 vol % N_2).

Effect of the Feed Gas Pressure on the VAm–VOH/PS Membrane Permselectivity

Figures 8 and 9 show the pure gas permselectivity of the VAm–VOH membrane with a VAm fraction of 54.8%. As shown in Figure 8, the CO_2 permeance was much higher than that of N_2 and CH_4. With increasing feed gas pressure, the CO_2 permeance decreased gradually, although the N_2 and CH_4 permeances were very low and remained nearly constant with the feed gas pressure. Figure 9 shows that both the CO_2/N_2 and CO_2/CH_4 ideal selectivity declined with increasing feed gas pressure.

The transport behavior shown in Figures 8 and 9 implied that the CO_2-transport mechanism was different from those of N_2 and CH_4. To the best of our knowledge, N_2 and CH_4 permeated the nonporous polymeric membrane with the solution–diffusion mechanism. According to the solution–diffusion mode, the gas permeance was independent of pressure.

The CO_2-transport behavior was very consistent with the facilitated transport mechanism. At a low feed gas pressure, the CO_2 permeance was extremely high and was dominated by the CO_2-carrier complex permeation. With increasing pressure, the carrier (primary amino group) was gradually saturated by CO_2. As a result, the facilitated transport contribution to the CO_2 permeance dropped with the feed gas pressure. At high pressures, the CO_2 permeance reached a nearly constant value because the primary contribution to CO_2 permeation was due to solution diffusion.

Figures 10–13 show the CO_2/N_2 and CO_2/CH_4 mixed-gas permselectivity of the VAm–VOH membrane. Similar to Figures 8 and 9, in the mixed-gas test, the CO_2 permeances were much

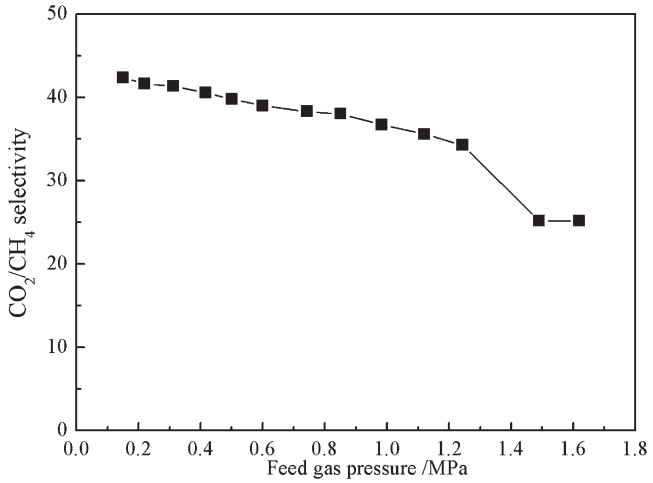

Figure 13. Effects of the feed gas pressure on the CO_2/CH_4 selectivity of the VAm–VOH/PS membrane with a 54.8% VAm fraction tested with a CO_2/CH_4 gas mixture (10 vol % CO_2 and 90 vol % CH_4).

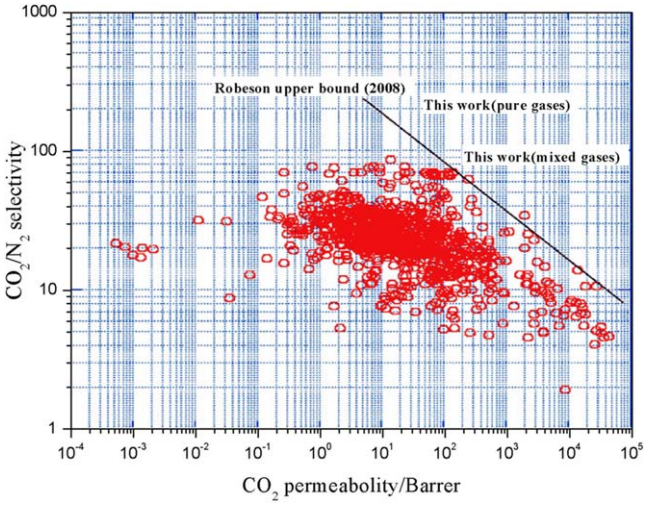

Figure 14. Comparison of the CO_2 permeability and CO_2/N_2 selectivity with the Robeson upper bound. [Color figure can be viewed in the online issue, which is available at wileyonlinelibrary.com.]

higher than the permeances of N_2 and CH_4 and decreased with pressure. The CO_2-transport behavior agreed with the facilitated transport mechanism. The N_2 and CH_4 permeances were extremely low with a slight change, and this was in accordance with the solution–diffusion mechanism.

As also shown in Figures 10–13, the CO_2 permeance in the mixed-gas test was slightly lower than that of the pure gas, whereas the N_2 and CH_4 permeances were higher than that of the pure gas. This phenomenon was attributed to the coupling effects between CO_2 and slow gas (e.g., N_2, CH_4). In the mixed-gas testing, CO_2 dissolved in the membrane, and this led to the larger mobility of the polymer chains. The increase in the polymer chain mobility promoted the diffusion of N_2 and CH_4.[15,37] Because of the competition between the slow gas and CO_2 for both sorption sites and diffusion pathways in the polymer matrix,[38] the CO_2 permeance of the mixed gas was slightly lower than that of the pure gas.

Figure 14 shows a comparison of the membrane performance in this study with other membranes listed by Robeson[39] in 2008. The CO_2 permeability in this study is calculated by the multiplication of the CO_2 permeance and the CO_2/N_2 separation layer thickness (ca. 4.8 μm). The highest CO_2 permeability was about 800–1200 Barrer [1 Barrer = 1 $\times$ 10^{-10} cm^3(STP) cm cm^{-2} s^{-1} $cmHg^{-1}$], whereas the selectivities were 170 and 62 for the pure gas and mixed gases, respectively. As shown in Figure 14, the permselectivity of the VAm–VOH/PS membrane in this study was higher than the Robeson upper bound.

Table II represents a comparison of the VAm–VOH/PS membrane with reported fixed-carrier membranes with primary amino groups as carriers. As shown in Table II, the VAm–VOH/PS membrane displayed a higher CO_2 permeance than the pure PVAm membrane and its blend membrane. For the membranes in refs. 9 and 35, the membrane contained some mobile carriers (ie. potassium salt of 2-aminoisobutyric acid (AIBA-K) and ethylenediamine), and this gave the membranes very high CO_2 permselectivities.

Table II. Comparison of Membrane Performance with Literature Results

Membrane	Pressure (MPa)	Feed gas	Thickness (μm)	CO_2 Permeance (GPU)	Selectivity	Reference
PVAm/PSf	0.12	10 % CO_2, 90% N_2	1.2	102	197	8
PEI-PVA	0.11	N/A	200	3.9	230	7
PVAm-PEG/PSf	0.26	10%CO_2, 90%CH_4	10	5.8	63	15
PAAm-PVA/PSf	0.1	10%CO_2, 90%CH_4	0.65	4	8 (RH=0.4)	16
				55	35 (RH=0.9)	
PVA/PAAm/AIBA-K	0.2	20 % CO_2,40 %H_2 and 40 % N_2	70	230	1800 (CO_2/N_2)	9
					450 (CO_2/H_2)	
PVAm-EDA/PSf	0.11	20% CO_2, 80% N_2	0.5	607	109	35
VAm-VOH/PSf	0.15	20% CO_2, 80% N_2	4	202	61.3	This work
VAm-VOH/PSf	0.15	Pure CO_2 and N_2	4	264	170	This work

RH is the relative humidity of testing gas.

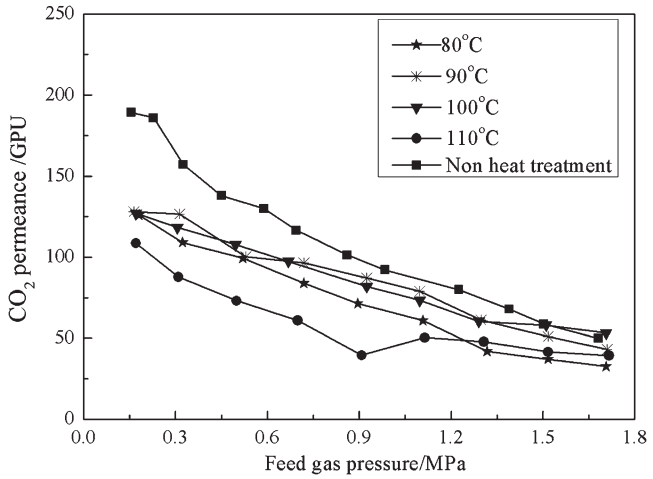

Figure 15. Effects of the heat-treatment temperature on the CO_2 permeance of the VAm–VOH/PS membrane with a 54.8% VAm fraction tested with a CO_2/N_2 gas mixture (20 vol % CO_2 and 80 vol % N_2).

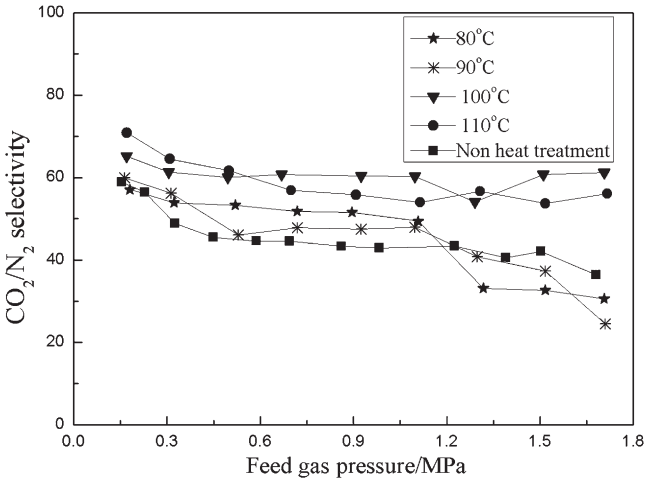

Figure 17. Effects of the heat-treatment temperature on the CO_2/N_2 selectivity of the VAm–VOH/PS membrane with a 54.8% VAm fraction tested with a CO_2/N_2 gas mixture (20 vol % CO_2 and 80 vol % N_2).

Effects of the Heat Treatment

Figures 15–17 show the effects of the heat-treatment temperature on the membrane gas-separation performance. The results indicate that the heat treatment had a notable effect on the membrane performance. Both the CO_2 and N_2 permeances decreased with increasing heat-treatment temperature, whereas the CO_2/N_2 selectivity showed a tendency to increase. At low pressures (0.01–0.9 MPa), the CO_2 permeance decreased significantly with increasing annealing temperature. When the pressure was higher than 1.2 MPa, the effect of the annealing temperature on the CO_2 permeance was not as significant as in the low-pressure region. At 0.14–0.15 MPa, the CO_2 permeance of the membrane that was heat-treated at 100°C was only 67% of that of the non-heat-treated membrane. When the feed gas pressure was increased to 1.68–1.7 MPa, the CO_2 permeance of the non-heat-treated membrane dropped to 49 GPU, whereas the CO_2 permeance of the 100°C heat-treated membrane dropped to 53 GPU (and was slightly higher than that of the non-heat-treated membrane). This indicated that the heat-treated membrane could withstand higher pressures. Compared with CO_2, the N_2 permeance drop with annealing temperature was more notable. The N_2 permeance of the membrane that was heat-treated at 110°C was only 50% of that of the non-heat-treated membrane.

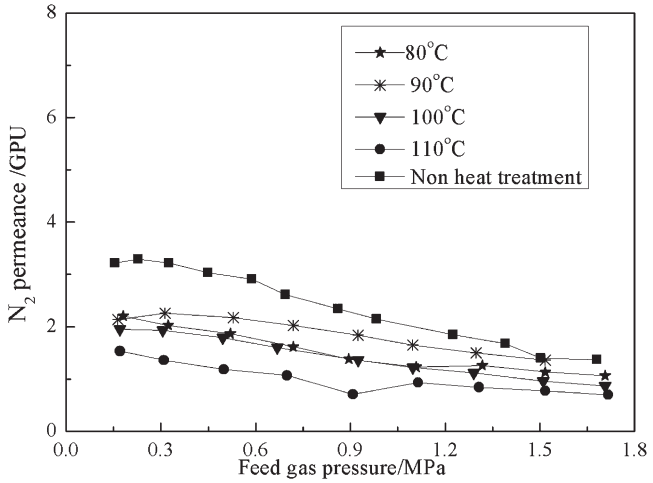

Figure 16. Effects of the heat-treatment temperature on the N_2 permeance of the VAm–VOH/PS membrane with a 54.8% VAm fraction tested with a CO_2/N_2 gas mixture (20 vol % CO_2 and 80 vol % N_2).

The gas permeances drop was attributed to rearrangement of molecular chains.[40] Generally, polymer chains become more ordered as the chain-packing density increases after thermal annealing.[40,41] With increasing annealing temperature, the membrane became denser, and this resulted in a lower gas permeance. As discussed before, CO_2 permeated the membrane according to the facilitated transport mechanism, whereas N_2 followed the solution–diffusion mechanism. The dominating factor for CO_2 permeation was the carrier in the membrane. As for N_2, the major factors were the solubility and diffusion coefficient. During the heat-treatment process, the carrier content did not change, whereas the membrane chain packing became denser. The densely packed chain structure led to difficulty in gas diffusion and a lower diffusion coefficient. As a result, heat treatment had a more significant effect on the permeation of N_2.

It has to be emphasized that there was an optimal heat-treatment temperature according to the selectivity improvement. When the annealing temperature was higher than 100°C, the CO_2/N_2 selectivity did not increase obviously with further increases in the annealing temperature, whereas the CO_2 permeance decreased dramatically. The reason for the CO_2 permeance drop may have been the oxidization of the amino group. At high temperatures, the amino group could be oxidized by the oxygen. The oxidization of the amino group led to the carrier content decrease and the CO_2 permeance drop. Therefore, the optimal annealing temperature was 100°C.

CONCLUSIONS

A VAm–VOH copolymer was synthesized, and VAm–VOH/PS composite membranes were prepared. The effects of the feed gas pressure, copolymer composition, and heat treatment on

the membrane gas permselectivity were investigated with CO_2, N_2, and CH_4 pure gases and mixed gases.

The primary amino groups in VAm–VOH reacted reversibly with CO_2, and this facilitated the permeation of the CO_2, N_2, and CH_4 through the membrane with the solution–diffusion mechanism.

Both the CO_2 permeance and CO_2/N_2 selectivity had maxima with increasing VAm fraction in the copolymer. The membrane with the VAm fraction of 54.8% possessed the highest CO_2 permeance of 189.4 GPU and an CO_2/N_2 selectivity of 58.9. This gas-transport phenomena was attributed to the carrier content, crystallization, and intermolecular hydrogen bonding.

The effects of the heat-treatment temperature on the membrane performance were investigated. Because of the denser chain packing after heat treatment, both the CO_2 and N_2 permeances decreased with increasing heat-treatment temperature, whereas the CO_2/N_2 selectivity increased. The optimal heat-treatment temperature for the VAm–VOH/PS membrane in this study was 100°C. At a feed gas pressure of 0.92 MPa, the membrane heat-treated at 100°C displayed a CO_2 permeance of 82 GPU and a CO_2/N_2 selectivity of 60.4.

ACKNOWLEDGMENTS

This work was supported by the Natural Science Foundation of China (contract grant number 21206131) and the National Basic Research Program (contract grant number 2009CB219906).

REFERENCES

1. Belaissaoui, B.; Cabot, G.; Cabot, M.-S.; Willson, D.; Favre, E. *Energy* **2012**, *38*, 167.
2. Belaissaoui, B.; Le Moullec, Y.; Willson, D.; Favre, E. *J. Membr. Sci.* **2012**, *415*, 424.
3. Deng, L.; Hägg, M.-B. *Int. J. Greenhouse Gas Control* **2010**, *4*, 638.
4. He, X.; Hägg, M.-B. *J. Membr. Sci.* **2011**, *378*, 1.
5. Luis, P.; Van Gerven, T.; Van der Bruggen, B. *Prog. Energy Combust.* **2012**, *38*, 419.
6. Dong, C. M.; Wang, Z.; Yi, C. H.; Wang, S. C. *J. Appl. Polym. Sci.* **2006**, *101*, 1885.
7. Matsuyama, H.; Terada, A.; Nakagawara, T.; Kitamura, Y.; Teramoto, M. *J. Membr. Sci.* **1999**, *163*, 221.
8. Sandru, M.; Kim, T.-J.; Hägg, M.-B. *Desalination* **2009**, *240*, 298.
9. Zou, J.; Ho, W. S. W. *J. Membr. Sci.* **2006**, *286*, 310.
10. Yoshikawa, M.; Ezaki, T.; Sanui, K.; Ogata, N. *J. Appl. Polym. Sci.* **1988**, *35*, 145.
11. Yoshikawa, M.; Fujimoto, K.; Kinugawa, H.; Kitao, T.; Kamiya, Y.; Ogata, N. *J. Appl. Polym. Sci.* **1995**, *58*, 1771.
12. Kim, T.-J.; Li, B.; Hägg, M.-B. *J. Polym. Sci. Part B: Polym. Phys.* **2004**, *42*, 4326.
13. Deng, L.; Kim, T.-J.; Hägg, M.-B. *Desalination* **2006**, *199*, 523.
14. Hussain, A.; Hägg, M.-B. *J. Membr. Sci.* **2010**, *359*, 140.
15. Yi, C. H.; Wang, Z.; Li, M.; Wang, J. X.; Wang, S. C. *Desalination* **2006**, *193*, 90.
16. Cai, Y.; Wang, Z.; Yi, C.; Bai, Y.; Wang, J.; Wang, S. *J. Membr. Sci.* **2008**, *310*, 184.
17. Yu, X.; Wang, Z.; Zhao, J.; Yuan, F.; Li, S.; Wang, J.; Wang, S. *Chin. J. Chem. Eng.* **2011**, *19*, 821.
18. Du, R.; Chakma, A.; Feng, X. *J. Membr. Sci.* **2007**, *290*, 19.
19. Zhang, Y.; Wang, Z.; Wang, S. C. *J. Appl. Polym. Sci.* **2002**, *86*, 2222.
20. Wang, Z.; Yi, C. H.; Zhang, Y.; Wang, J. X.; Wang, S. C. *J. Appl. Polym. Sci.* **2006**, *100*, 275.
21. Zhang, Y.; Wang, Z.; Wang, S. C. *Desalination* **2002**, *145*, 385.
22. Zhang, Y.; Wang, Z.; Zhao, J.; Wang, J. X.; Wang, S. C. *Chin. Chem. Lett.* **2006**, *17*, 277.
23. Patel, N. P.; Miller, A. C.; Spontak, R. *J. Adv. Mater.* **2003**, *15*, 729.
24. Lin, H.; Freeman, B. D. *J. Mol. Struct.* **2005**, *739*, 57.
25. Liu, L.; Chakma, A.; Feng, X. S. *J. Membr. Sci.* **2004**, *235*, 43.
26. Liu, L.; Chakma, A.; Feng, X. S. *Chem. Eng. J.* **2004**, *105*, 43.
27. Okamoto, K.; Fujii, M.; Okamyo, S.; Suzuki, H.; Tanaka, K.; Kita, H. *Macromolecules* **1995**, *28*, 6950.
28. Nistor, C.; Shishatskiy, S.; Popa, M.; Nunes, S. P. *Sep. Sci. Technol.* **2009**, *44*, 3392.
29. Gu, L.; Zhu, S.; Hrymak, A. N. *J. Appl. Polym. Sci.* **2002**, *86*, 3412.
30. Wang, Z.; McDonald, A. G.; Westerhof, R. J. M.; Kersten, S. R. A.; Cuba-Torres, C. M.; Ha, S.; Pecha, B.; Garcia-Perez, M. *J. Anal. Appl. Pyrol.* **2013**, *100*, 56.
31. Tong, Y.-Y.; Dong, Y.-Q.; Du, F.-S.; Li, Z.-C. *J. Polym. Sci. Part A: Polym. Chem.* **2009**, *47*, 1901.
32. Hu, S. Y.; Zhang, Y.; Lawless, D.; Feng, X. *J. Membr. Sci.* **2012**, 417–418, *34*.
33. Hagg, M. B.; Quinn, R. *MRS Bull.* **2006**, *31*, 750.
34. Zhao, Y.; Winston Ho, W. S. *J. Membr. Sci.* **2012**, 415–416, *132*.
35. Yuan, S.; Wang, Z.; Qiao, Z.; Wang, M.; Wang, J.; Wang, S. *J. Membr. Sci.* **2011**, *378*, 425.
36. Boas, U.; Karlsson, A. J.; de Waal, B. F. M.; Meijer, E. W. *J. Org. Chem.* **2001**, *66*, 2136.
37. Zhang, Y.; Wang, Z.; Wang, S. C. *Chin. J. Chem. Eng.* **2002**, *10*, 570.
38. Shen, J.; Qiu, J.; Wu, L.; Gao, C. *Sep. Purif. Technol.* **2006**, *51*, 345.
39. Robeson, L. M. *J. Membr. Sci.* **2008**, *320*, 390.
40. Ismail, A. F.; Lorna, W. *Sep. Purif. Technol.* **2003**, *30*, 37.
41. Duthie, X.; Kentish, S.; Pas, S. J.; Hill, A. J.; Powell, C.; Nagai, K.; Stevens, G.; Qiao, G. *J. Polym. Sci. Part B: Polym. Phys.* **2008**, *46*, 1879.